

## Variation of magnetization and the Landé $g$ factor with thickness in Ni–Fe films

J. P. Nibarger,<sup>a)</sup> R. Lopusnik, Z. Celinski,<sup>b)</sup> and T. J. Silva  
National Institute of Standards and Technology, Boulder, Colorado 80305

(Received 17 February 2003; accepted 1 May 2003)

We have measured the Landé  $g$  factor, the effective magnetization  $M_{\text{eff}}$ , the uniaxial anisotropy  $H_k$ , and the Gilbert damping parameter  $\alpha$ , as a function of Permalloy film thickness from 2.5 to 50 nm. We used a pulsed inductive microwave magnetometer capable of generating dc bias fields of 35.2 kA/m (440 Oe). A significant decrease in  $g$  is observed with decreasing thickness below 10 nm. Also,  $M_{\text{eff}}$  decreases with decreasing thickness consistent with a surface anisotropy constant of  $0.196 \pm 0.025$  mJ/m<sup>2</sup>. The decrease in  $g$  can arise from the orbital motion of the electrons at the interface not being quenched by the crystal field. We also compare our data to a model of an effective  $g$  factor suggesting that the decrease in  $g$  factor might also stem from the Ni–Fe interface with a Ta underlayer. [DOI: 10.1063/1.1588734]

As the magnetic-data-storage industry develops disk drives with data transfer rates approaching 1 Gbit/s, understanding the underlying dynamics of the soft magnetic components used in recording heads becomes increasingly important. Two important material parameters that govern the response and precessional frequency of a magnetic film are the effective magnetization  $M_{\text{eff}}$  and the Landé  $g$  factor.  $M_{\text{eff}}$  affects the dynamics by generating internal demagnetizing fields during the switching process that greatly accelerate the precessional motion. The Landé  $g$  factor sets the proportionality of angular momentum and magnetic moment for the individual spins that results in precessional motion. For state-of-the-art heads with exceedingly small magnetic layer thicknesses, interfaces play a large role, and understanding the effect of interfaces on  $M_{\text{eff}}$  and  $g$  is crucial for the engineering of high-performance recording systems. The thickness dependence of  $M_{\text{eff}}$  and  $g$  in the case of thin Permalloy films was first measured by ferromagnetic resonance.<sup>1</sup>

We demonstrate the ability of a pulsed inductive microwave magnetometer (PIMM) to measure simultaneously the effective magnetization  $M_{\text{eff}}$ , the uniaxial anisotropy  $H_k$ , and the spectroscopic Landé  $g$  factor, at high dc bias fields. This is done for a thickness series of Permalloy films ( $\text{Ni}_{81}\text{Fe}_{19}$ ) ranging from 2.5 to 50 nm. By applying large dc fields [35.2 kA/m (440 Oe)] along the easy axis of the sample during measurements, we are able to extract  $M_{\text{eff}}$ ,  $g$ , and  $H_k$  simultaneously using a nonlinear, three-parameter fit. This is in contrast to most permeameters, which require a separate measurement of  $M_{\text{eff}}$ . In addition, the Gilbert damping parameter  $\alpha$ , was extracted as a function of thickness.

Polycrystalline Permalloy films were deposited on 1 cm $\times$ 1 cm $\times$ 100  $\mu\text{m}$  (0001) oriented sapphire coupons. The sapphire substrates were cleaned using ion milling in Ar/O<sub>2</sub> and Ar atmospheres to remove contaminants. Then, a dc magnetron operating in an Ar atmosphere at 0.533 Pa (4 mTorr) was used to sputter a 5 nm Ta adhesion layer. Permalloy films of 2.5, 5, 7.5, 10, 15, 25, or 50 nm thicknesses

were then deposited followed by a 5 nm capping layer of Cu to protect the Permalloy against oxidation. Samples were grown in a 20 kA/m (250 Oe) external magnetic field to induce uniaxial anisotropy. Photolithography and a nitric acid etch was used to pattern a 3 mm $\times$ 3 mm square in the center of the Permalloy coupon. The reduced sample area was required to guarantee high uniformity of the dc bias field across the area of the sample during measurements. Figure 1 upper inset shows typical hard- and easy-axis hysteresis loops of the unpatterned 50-nm-thick sample characterized using an induction-field loop to verify their quality.

Samples were measured by use of a PIMM.<sup>2</sup> A coplanar waveguide of 50  $\Omega$  impedance and 100  $\mu\text{m}$  center conductor was used. The easy axis of the sample was aligned parallel to the center conductor, as shown in the lower inset of Fig. 1. A commercial pulse generator provided 10 V pulses, with 50 ps

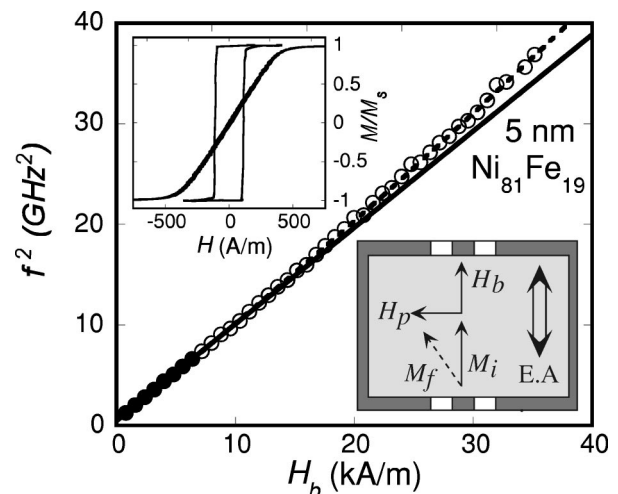


FIG. 1. Frequency squared as a function of bias field for a 5 nm sample; the error bars are the size of the circles. Data for bias field 0.8–7.16 kA/m (10–90 Oe) are shown with filled-in circles and fitted linearly with a solid line to demonstrate the deviation from linearity of the data at high bias fields. All of the data were fitted with Eq. (1) (dashed line). Lower inset shows the measurement geometry used for pulsed inductive microwave magnetometer measurements, with the easy axis of the sample parallel to the applied dc bias field. Upper inset shows induction field loop measurements of the unpatterned 50 nm thick sample showing the easy- and hard-axis hysteresis loops with easy-axis squareness of 0.99.

<sup>a)</sup>Electronic mail: nibarger@boulder.nist.gov

<sup>b)</sup>Present address: Department of Physics, University of Colorado at Colorado Springs, Colorado Springs, CO 80918.

rise times and 10 ns durations. The pulsed field  $H_p$ , was oriented along the hard axis of the sample. The nominal field pulse amplitudes were found by the use of the Karlquist equation for fields from a current strip<sup>3</sup> to be 800 A/m (10 Oe). The Permalloy films were placed facing the waveguide. To prevent shorting of the coplanar waveguide a thin layer of photoresist ( $<1 \mu\text{m}$ ) was spin coated onto the sample.

Static longitudinal bias fields ( $H_b$  in Fig. 1 lower inset), ranging from 0.8 to 35.2 kA/m (10 to 440 Oe), were generated by an electromagnet with soft iron pole pieces and a circular yoke.<sup>4</sup> Field calibration was performed to avoid any effects of remanence and allowed the fields to be set with an uncertainty of 1%. Field uniformity along the waveguide was better than 1% over a length of 4 mm. Coil resistance was monitored to determine if any heating had occurred that could lead to field drift. If the resistance was more than 2.5% above room-temperature resistance, then data acquisition was temporarily stopped until the coils cooled.

Precessional response was measured with a 20 GHz-bandwidth digital sampling oscilloscope. The measured precession frequencies ranged from 1 to 6.5 GHz and were well within the bandwidth of the detection system.<sup>2</sup> A background response was obtained with an applied saturation field of 2.4 kA/m (30 Oe) along the hard axis and zero field along the easy axis. The precessional dynamics was extracted by subtracting the measured and background signals.

The induced voltage of the precessional response measured in the time domain was converted into frequency spectra by fast Fourier transform for further analysis. The Gilbert damping parameter  $\alpha$ , was extracted from the full width at half maximum of the imaginary part of the spectrum  $\Delta\omega$ , such that:  $\alpha \approx \Delta\omega / (\gamma\mu_0 M_{\text{eff}})$ .<sup>5</sup> The resonance of the signal was extracted from the zero crossing of the real part of the spectrum. The resonance frequency as a function of bias field can be described by the Kittel formula for a thin film<sup>6</sup>

$$\omega_0^2 = \left( \frac{g\mu_B\mu_0}{\hbar} \right)^2 (M_{\text{eff}} + H_k + H_b)(H_k + H_b), \quad (1)$$

where  $\mu_B$  is the Bohr magneton,  $\hbar$  is Planck's constant divided by  $2\pi$ , and  $\mu_0$  is the permeability of free space. A simultaneous three-parameter fit of  $\omega_0^2$  vs  $H_b$  can be used to extract  $M_{\text{eff}}$ ,  $g$ , and  $H_k$ . We emphasize that a three-parameter fit is possible only when a sufficiently large field range is used such that terms in Eq. (1) quadratic in bias field are no longer negligible. Fortunately, the applied dc fields need not be as large as  $M_{\text{eff}}$  for the nonlinearity in  $\omega_0^2$  vs  $H_b$  to be measurable. Since surface anisotropies may exist for very thin magnetic films, the demagnetizing fields induced by out-of-plane motion of the magnetization vector differs from the saturation magnetization by the usual surface anisotropy term<sup>7</sup>

$$\mu_0 M_{\text{eff}} = \mu_0 M_s - \frac{2K_s}{M_s\delta}, \quad (2)$$

where  $\delta$  is the film thickness and  $K_s$  is the average anisotropy, consisting of the sum of the Cu/NiFe and Ta/NiFe interface surface anisotropies.

Figure 1 is a plot of frequency squared,  $f^2 = (\omega/2\pi)^2$  as a function of longitudinal bias field for a 5-nm-thick film. The uncertainty in  $f^2$  is found to vary from 5% at 1 GHz<sup>2</sup> to

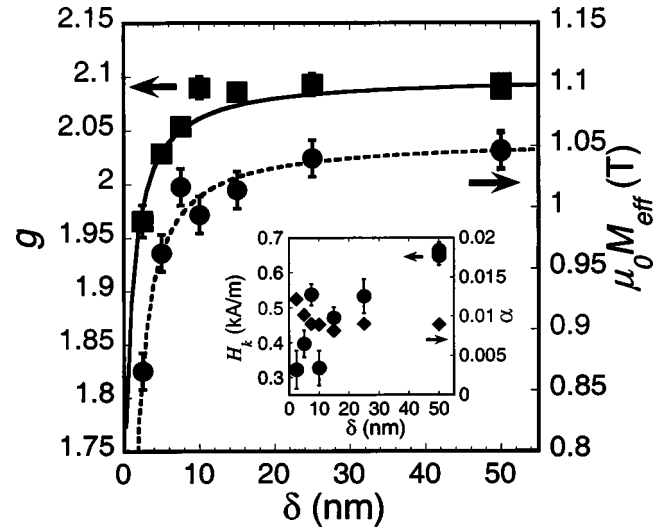


FIG. 2.  $\mu_0 M_{\text{eff}}$  and  $g$  as a function of thickness,  $\delta$ . Inset shows  $H_k$  and  $\alpha$  as a function of  $\delta$ . The  $\alpha$  values plotted are with 8 kA/m longitudinal bias field applied.  $\mu_0 M_{\text{eff}}$  was fitted to Eq. (2) (dashed line), yielding  $\mu_0 M_s = 1.0553$  T and  $K_s = 0.196$  mJ/m<sup>2</sup>. The measured  $g$  factor is compared to Eq. (7) (solid line) where  $T_{\text{Ta/NiFe}} = 0.6$  nm (see Ref. 12),  $T_{\text{Cu/NiFe}} = 0.4$  nm,  $g_{\text{NiFe}} = 2.1$  (see Refs. 1, and 13)  $g_{\text{Ta/NiFe}} = 1.58$  (see Ref. 14),  $g_{\text{Cu/NiFe}} = 2.05$  (see Ref. 15).

0.8% at 40 GHz<sup>2</sup>. The data can be fit using Eq. (1) (dashed line) to yield values of  $M_{\text{eff}}$ ,  $g$ , and  $H_k$ . To highlight the deviation from linearity, data for 0.8–7.2 kA/m (10–90 Oe) bias fields (shown with filled-in circles) were fitted to a linear function of  $H_b$ , with the fit extrapolated to high fields. The data are as much as 8% greater than the linear extrapolation from low field data, showing the magnitude of the nonlinearity to be fitted in the extraction of  $M_{\text{eff}}$ ,  $g$ , and  $H_k$ . For each thickness, multiple measurements were made to determine statistics for repeatability and to decrease noise through averaging. Due to the 1% uncertainty in bias fields, a systematic error of 2.5% for  $g$ , 4% for  $M_{\text{eff}}$ , and 12% error in  $H_k$  are presumed. Results for  $M_{\text{eff}}$  and  $g$  as a function of thickness  $\delta$ , are shown in Fig. 2.  $H_k$  and  $\alpha$  as a function of thickness is shown in Fig. 2 inset. The  $\alpha$  values plotted are from data with an 8 kA/m longitudinal bias field.

The Gilbert damping parameter,  $\alpha$ , increased with decreasing film thickness, consistent with previous measurements in Permalloy.<sup>8</sup>  $H_k$  appears to vary randomly with an average value of  $408 \pm 40$  A/m ( $5.1 \pm 0.5$  Oe) for  $2.5 < \delta < 15$  nm, with no observable trend within the error bars for the measurement. However, both  $M_{\text{eff}}$  and  $g$  decrease significantly with decreasing film thickness below 10–20 nm. In practical terms, the reduction in  $M_{\text{eff}}$  and  $g$  is a decrease in the intrinsic ferromagnetic resonance frequency for the thinnest Permalloy by 27% relative to the thickest films, equivalent to a shift in the precessional frequency of 230 MHz.

Values obtained for  $\mu_0 M_{\text{eff}}$  with the PIMM are consistent with values obtained from an alternating gradient magnetometer (AGM). For 50 and 25 nm sample thicknesses the AGM measured values of  $\mu_0 M_{\text{eff}}$  were 1.0630 and 1.0180 T, respectively, compared to 1.0462 and 1.0398 T, respectively, from the PIMM measurements. The observed decrease in  $\mu_0 M_{\text{eff}}$  with decreasing thickness is consistent with a surface anisotropy contribution given by Eq. (2). A fit to Eq. (2) is shown in Fig. 2 as a dashed line.  $K_s$  is  $0.196 \pm 0.025$  mJ/m<sup>2</sup>

and  $\mu_0 M_s$  is  $1.0553 \pm 0.046$  T. The error in  $K_s$  and  $\mu_0 M_s$  accounts for both random error and the uncertainty of 1% for the bias field.

In general, both the orbital and spin angular momentum contribute to the total angular momentum of an electron. As such, the  $g$  factor may be written as

$$g = \frac{2m_e}{e} \frac{\mu_S + \mu_L}{\langle S \rangle + \langle L \rangle}, \quad (3)$$

where  $\mu_S$  and  $\mu_L$  are the contributions to the electron magnetic moment due to the spin and orbital components, respectively. For a symmetric crystal lattice, the orbital motion of the electron during gyromagnetic precession is quenched by the crystal field, i.e.,  $\langle L \rangle = 0$ . Thus, the orbital contribution to the electron angular momentum is zero even though the orbital contribution to the magnetic moment is nonzero resulting in a  $g$  factor that is always greater than two.<sup>9</sup>

$$g = \frac{2m_e}{e} \frac{\mu_S + \mu_L}{\langle S \rangle} = 2 \left( 1 + \frac{\mu_L}{\mu_S} \right). \quad (4)$$

However, the orbital motion is not entirely quenched at surfaces and interfaces where the crystal field is no longer symmetric since the interface breaks inversion symmetry. Under such circumstances, the orbital motion can still contribute to the gyromagnetic motion. Equation (3) can then be written as

$$g = \frac{2m_e}{e} \frac{\mu_S}{\langle S \rangle} \frac{\left( 1 + \frac{\mu_L}{\mu_S} \right)}{\left( 1 + \frac{\langle L \rangle}{\langle S \rangle} \right)} \approx 2 \left( 1 - \frac{\mu_L}{\mu_S} \right), \quad (5)$$

since  $\langle S \rangle = \mu_S m_e / e$ ,  $\langle L \rangle = 2\mu_L m_e / e$  and expanding the Taylor's series to first order. Thus, surfaces and interfaces allow for the possibility that the  $g$  factor is less than 2. Two physical mechanisms are plausible sources for this interface effect. First, the orbital motion is not quenched by the crystal field, i.e.,  $\langle L \rangle \neq 0$ . In addition, material mixing at the interface could alter the  $g$  factor. We can model the latter hypothesis of interface mixing by relying on the concept of an effective  $g$  factor,  $g_{\text{eff}}$ , first proposed by Wangness<sup>10,11</sup>

$$\frac{\rho_{\text{NiFe}} V_{\text{NiFe}} + \rho_{\text{Ta/NiFe}} V_{\text{Ta/NiFe}} + \rho_{\text{Cu/NiFe}} V_{\text{Cu/NiFe}}}{g_{\text{eff}}} = \frac{\rho_{\text{NiFe}} V_{\text{NiFe}}}{g_{\text{NiFe}}} + \frac{\rho_{\text{Ta/NiFe}} V_{\text{Ta/NiFe}}}{g_{\text{Ta/NiFe}}} + \frac{\rho_{\text{Cu/NiFe}} V_{\text{Cu/NiFe}}}{g_{\text{Cu/NiFe}}}, \quad (6)$$

where  $\rho_i$ ,  $V_i$ , and  $g_i$  are the spin density, volume, and  $g$  factor for each of the respective layers or interfaces ( $i = \text{NiFe}, \text{Ta/NiFe}, \text{Cu/NiFe}$ ). The volume  $V_i$  may be set equal to the thickness  $t_i$  since the interface area is the same for each layer. Equation (6) can be rewritten as a function of the thickness of the Permalloy film,  $\delta$ :

$$g_{\text{eff}}(\delta) = \frac{\delta + t_{\text{Ta/NiFe}} + t_{\text{Cu/NiFe}}}{\frac{\delta}{g_{\text{NiFe}}} + \frac{t_{\text{Ta/NiFe}}}{g_{\text{Ta/NiFe}}} + \frac{t_{\text{Cu/NiFe}}}{g_{\text{Cu/NiFe}}}}. \quad (7)$$

We assume that the spin density  $\rho_i$  is invariant through the film thickness and that reasonable assumptions for the Cu/NiFe and Ta/NiFe interface thickness and the  $g$ -factors for the films and interfaces can be made.

The mixing at Ta/NiFe interfaces has been well studied for magnetic random access memory (MRAM) and giant magnetoresistance applications. Kowalewski *et al.*<sup>12</sup> found the interface thickness for unannealed samples to be 0.6 nm. The thickness of the Cu/NiFe interfaces is approximately two monolayers (0.4 nm). The measured  $g$  factor for NiFe from this experiment for the thickest films is 2.1, which is consistent with other published values (2.08,<sup>1</sup> 2.08,<sup>13</sup> and 2.17).<sup>13</sup> For the  $g$  factor at the Ta/NiFe interface, we make a very coarse approximation and use the Ta bulk value of 1.58.<sup>14</sup> Likewise, the  $g$  factor for Cu/NiFe is simply that of bulk Cu, 2.05,<sup>15</sup> a value not too different from that of bulk Permalloy. A plot of Eq. (7) with the earlier assumption is shown in Fig. 2 with no adjustable parameters. The calculated reduction in  $g$  with decreasing NiFe thickness is in large part the result of the Ta interface, which has a large orbital contribution to the moment.

This model works surprisingly well as an explanation for the thickness variation of  $g$ , in spite of the particularly crude assumptions made of uniform spin density and bulk values for the  $g$  factors at the various interfaces. These two assumptions stem from the presumption that ferromagnetism persists even in an intermixed atomic environment, though the orbital momentum contribution to the total angular momentum of the ferromagnetic spins is dominated by the electronic structure of the nonmagnetic constituent. We conclude that either the orbital motion at the interface is not quenched by the crystal field, i.e.,  $\langle L \rangle \neq 0$ , or that interfacial mixing of ferrous and nonferrous materials, or some combination of these two effects can explain the significant deviations of the precessional dynamics in thin Permalloy films from that predicted from bulk values of the  $g$  factor.

The authors would like to thank T. Kos for technical assistance. Z.C. acknowledges the financial support from ARO (Grant No. DAAG19-00-1-0146).

<sup>1</sup>M. H. Seavey and P. E. Tannenwald, J. Appl. Phys. **29**, 292 (1958).

<sup>2</sup>T. J. Silva, C. S. Lee, T. M. Crawford, and C. T. Rogers, J. Appl. Phys. **85**, 7849 (1999), A. B. Kos, T. J. Silva, and P. Kabos, Rev. Sci. Instrum. **73**, 3563 (2002).

<sup>3</sup>O. Karlquist, Trans. R. Inst. Tech. Stockholm **86**, 3 (1954).

<sup>4</sup>A. B. Kos, J. P. Nibarger, R. Lopusnik, T. J. Silva, and Z. Celinski, J. Appl. Phys. **93**, 7068 (2003).

<sup>5</sup>J. P. Nibarger, R. Lopusnik, and T. J. Silva, Appl. Phys. Lett. **82**, 2112 (2003).

<sup>6</sup>C. Kittel, *Introduction to Solid State Physics*, 7th ed. (Wiley, New York, 1995).

<sup>7</sup>L. Néel, Compt. Rend. **238**, 3051468 (1953).

<sup>8</sup>S. Ingvansson, L. Ritchie, X. Y. Liu, Gang Xiao, J. C. Slonczewski, P. L. Trouilloud, and R. H. Koch, Phys. Rev. B **66**, 214416 (2002).

<sup>9</sup>S. Chikazumi, *Physics of Magnetism* (Krieger, Malabar, FL, 1964), p. 52.

<sup>10</sup>R. K. Wangness, Phys. Rev. **91**, 1085 (1953).

<sup>11</sup>M. Farle, A. N. Anisimov, K. Beberschke, J. Langer, and H. Maletta, Europhys. Lett. **49**, 658 (2000).

<sup>12</sup>M. Kowalewski, W. H. Butler, N. Moghadam, G. M. Stocks, T. C. Schulthess, K. J. Song, J. R. Thompson, A. S. Arrott, T. Zhu, J. Drewes, R. R. Katti, M. T. McClure, and O. Escorcia, J. Appl. Phys. **87**, 5732 (2000).

<sup>13</sup>R. M. Bozorth, *Ferromagnetism* (IEEE, New York, 1978).

<sup>14</sup>C. Schober and V. N. Antonov, Phys. Status Solidi B **143**, K31 (1987).

<sup>15</sup>G. E. Grechnev, N. V. Savchenko, I. V. Svehcharev, M. J. G. Lee, and J. M. Perz, Phys. Rev. B **39**, 9865 (1989).